

INTEGRATED CAPACITIVE MICROPHONE

Anca TOMESCU, Sorin ANTONIU, F.M.G. TOMESCU
Electrical Engineering Dept., POLITEHNICA University – Bucharest
 George Cătălin CAZANGIU

The effective capacitance of an integrated capacitive microphone is computed by a mixed approximate analytical method and finite element numerical method.

INTRODUCTION

Microdevices represent a subject of increasing interest due to their multiple applications in industry, medicine, military, and many other fields. The structure of microdevices is generally subjected to certain restrictions derived from their manufacturing process which uses integrated circuit technology. The devices based on the electric field are generally preferred to those based on the magnetic field, and capacitive microphones are thus a device of choice when miniaturisation of sound collecting is desired [1,2,3].

The design of an integrated capacitive microphone starts from a preliminary performance evaluation, aiming at establishing the range of the proper design and manufacturing requirements. In this respect, the evaluation of the effective capacitance of the microphone is quite important for both the overall performance evaluation and the design of appropriate amplification and post-processing equipment. A mixed approximate analytical and finite element numerical approach to the computation of the capacitance of an integrated capacitive microphone is proposed in this paper.

DEVICE MODEL AND SIMPLIFYING ASSUMPTIONS

The electrically active part of the capacitive microphone [4] is a capacitor consisting in a diaphragm electrode attached to the diaphragm and a hollow electrode attached to the hollow backplate of the microphone (fig. 1). Acoustic waves incident on the structure induce the vibration of the diaphragm and backplate and thus determine a change in the associated electric capacitance. In turn, when a polarisation voltage is applied between the capacitor plates, the capacitance variation induces a current which translates the acoustic vibrations into electric oscillations. The simplified model of the microphone consists in equally spaced holes and hollow-segmented backplate electrode above the continuous diaphragm electrode, for which the rough approximation of the capacitance is [1]

$$C_{\text{approx}} = \frac{\epsilon_0 \epsilon_d L^2}{\epsilon_d h_a + h_d} \left(1 - \frac{4a^2}{b^2} \right) .$$

This formula corresponds to the extremely simplified parallel-plate capacitor approximation, which ignores the stray field associated with the holes in the upper electrode and the fringe field around the electrodes, and is susceptible to refinements that are discussed in the following.

Some simplifying hypotheses are supposed to apply:

- 1°. The domain of the problem is electrically linear and piece-wise homogeneous;
- 2°. The exact manufacturing details and electric connections are ignored and the thickness of the capacitor electrodes is neglected;
- 3°. The inter-hole median planes and the hole median planes of the upper hollow electrode are taken as field planes.

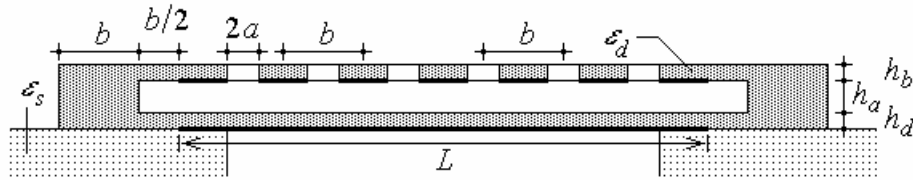


Fig. 1. Microphone structure

The repetitive structure of the capacitive microphone makes it sufficient to compute separately the contributions to the capacitance coming from: (1°) the electrode parts around an inner hole, (2°) the electrode parts around a marginal hole, and (3°) the electrode parts around a corner electrode. Thus, if N^2 is the number of holes in the upper electrode, and

$$L = (N + 1)b - 2a \quad ,$$

then the actual capacitance is

$$C = (N - 2)^2 C_{hole} + 4(N - 2)C_{marg} + 4C_{corner} \quad ,$$

where the notations are obvious.

The analytical approach to the computation of the effective capacitance [5,6,7] is based on the field line approximation by straight segments and circular arcs [8], which can be applied in three-dimensional and two-dimensional formulations. If $C_{lin X}$ is the capacitance per unit line in the $X = hole$ or $X = marg$ cases under the two-dimensional approximation, then the effective edge lengths corresponding to the three cases are found from the comparison with the three-dimensional approximation of the same structures,

$$C_{hole} = 4l_h C_{lin hole} \quad \Rightarrow \quad l_h = C_{hole} / 4C_{lin hole} \quad ,$$

$$C_{marg} = 2l_m (C_{lin hole} + C_{lin marg}) \quad \Rightarrow \quad l_m = C_{marg} / 2(C_{lin hole} + C_{lin marg}) \quad ,$$

$$C_{corner} = 2l_c \left(\frac{C_{lin hole}}{2} + \frac{3C_{lin marg}}{2} \right) \quad \Rightarrow \quad l_c = C_{corner} / (C_{lin hole} + 3C_{lin marg}) \quad .$$

The two-dimensional finite element numerical approach gives corresponding $C_{num X}$ values for the capacitance per unit length, whence the three-dimensional numerical approximations are obtained respectively as

$$C_{HOLE} = 4l_h C_{num hole} \quad ,$$

$$C_{MARG} = 2l_m (C_{num\ hole} + C_{num\ marg}) ,$$

$$C_{CORNER} = l_c (C_{num\ hole} + 3C_{num\ marg}) .$$

COMPUTATION OF THE ELECTRIC CAPACITANCES

The structures associated with an inner and a marginal hole in the two-dimensional analytical approximation are presented side by side in fig. 2 and the corresponding formulae (with $h_b = a$ for the sake of simplicity) are

$$C_{lin\ hole} = \frac{\epsilon_0 \epsilon_d (b - 2a)}{2(\epsilon_d h_a + h_d)} + \frac{2\epsilon_0 \epsilon_d}{\pi(\epsilon_d + 1)} \ln \left[1 + \frac{\pi(\epsilon_d + 1)a}{2(\epsilon_d h_a + h_d)} \right] ,$$

$$C_{lin\ marg} = C_{lin\ hole} + \frac{\epsilon_0 \epsilon_d (b - 3a)}{\epsilon_d h_a + h_d} + \frac{\epsilon_d \epsilon_s \epsilon_0}{\pi(\epsilon_d + \epsilon_s)} \ln \left[1 + \frac{\pi(\epsilon_d + \epsilon_s)}{\epsilon_s} \frac{h_b}{\epsilon_d h_a + h_d} \right] + \int_{h_b}^{b-3a} \frac{\epsilon_0 dx}{h_a + \frac{h_d}{\epsilon_d} + \frac{\epsilon_s + 1}{\epsilon_s} \pi x - 2 \frac{\epsilon_d - 1}{\epsilon_d} x \arcsin \frac{h_b}{x}} .$$

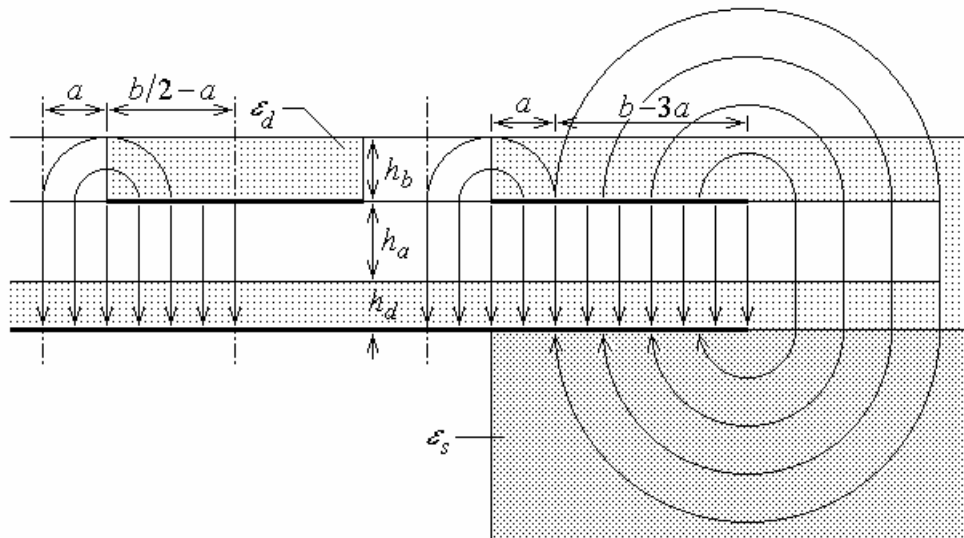


Fig. 2. Field line patterns for inner and marginal hole

The projections of domains covered by the three-dimensional analytical approximation are presented in fig. 3 and the corresponding formulae are [9]

$$C_{hole} = \frac{\epsilon_0 \epsilon_d}{\epsilon_d h_a + h_d} (b^2 - 4a^2) + 8\epsilon_0 \frac{4\epsilon_d (\epsilon_d h_a + h_d)}{\pi^2 (\epsilon_d + 1)^2} \left[1 + \frac{\pi (\epsilon_d + 1)a}{2 \epsilon_d h_a + h_d} \right] \ln \left[1 + \frac{\pi (\epsilon_d + 1)a}{2 \epsilon_d h_a + h_d} \right] ,$$

$$\begin{aligned}
 C_{marg} = & \frac{C_{hole}}{2} + \frac{\varepsilon_0 \varepsilon_d}{\varepsilon_d h_a + h_d} [b(b-a) - 2a^2] + \\
 & + \frac{\varepsilon_0 \varepsilon_d \varepsilon_s b}{\pi(\varepsilon_d + \varepsilon_s)} \ln \left[1 + \frac{\pi(\varepsilon_d + \varepsilon_s)}{\varepsilon_s} \frac{h_b}{\varepsilon_d h_a + h_d} \right] + \\
 & + \int_{h_b}^{b-3a} \frac{\varepsilon_0 b dx}{h_a + \frac{h_d}{\varepsilon_d} + \frac{\varepsilon_s + 1}{\varepsilon_s} \pi x - 2 \frac{\varepsilon_d - 1}{\varepsilon_d} x \arcsin \frac{h_b}{x}} + \\
 & + \int_{b-3a}^{b-a} \frac{\varepsilon_0 (b-4a) dx}{h_a + \frac{h_d}{\varepsilon_d} + \frac{\varepsilon_s + 1}{\varepsilon_s} \pi x - 2 \frac{\varepsilon_d - 1}{\varepsilon_d} x \arcsin \frac{h_b}{x}} + \\
 & + \int_0^{2a} \frac{\varepsilon_0 (4a - 2x) dx}{h_a + \frac{h_d}{\varepsilon_d} + \frac{\varepsilon_s + 1}{\varepsilon_s} \pi (b-3a+x) - 2 \frac{\varepsilon_d - 1}{\varepsilon_d} (b-3a+x) \arcsin \frac{h_b}{b-3a+x}} ,
 \end{aligned}$$

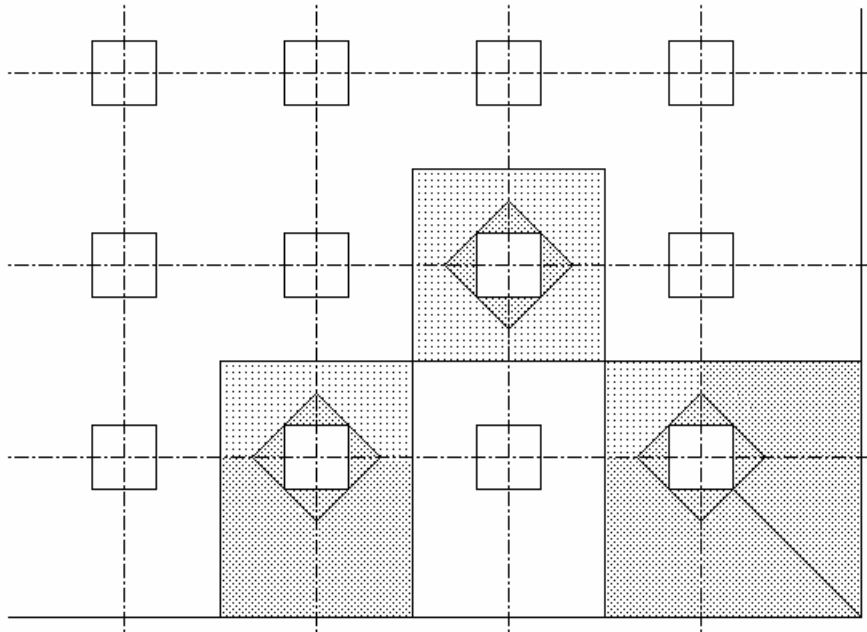


Fig. 3. Areas covered by the three-dimensional approximation

$$\begin{aligned}
 C_{corner} = & \frac{C_{hole}}{4} + C_{marg} + \frac{\varepsilon_0 \varepsilon_d}{\varepsilon_d h_a + h_d} [(b-a)^2 - a^2] + \\
 & + \frac{2\varepsilon_0 \varepsilon_d \varepsilon_s (b-a-h_b)}{\pi(\varepsilon_d + \varepsilon_s)} \ln \left[1 + \frac{\pi(\varepsilon_d + \varepsilon_s)}{\varepsilon_s} \frac{h_b}{\varepsilon_d h_a + h_d} \right] + \\
 & + \int_{h_b}^{b-3a} \frac{2\varepsilon_0 a dx}{h_a + \frac{h_d}{\varepsilon_d} + \frac{\varepsilon_s + 1}{\varepsilon_s} \pi x - 2 \frac{\varepsilon_d - 1}{\varepsilon_d} x \arcsin \frac{h_b}{x}} +
 \end{aligned}$$

$$\begin{aligned}
 & + \int_0^{b-2a-h_b} \frac{2\varepsilon_0(b-2a-h_b-x)dx}{h_a + \frac{h_d}{\varepsilon_d} + \frac{\varepsilon_s+1}{\varepsilon_s}\pi(h_b+x) - 2\frac{\varepsilon_d-1}{\varepsilon_d}(h_b+x)\arcsin\frac{h_b}{h_b+x}} + \\
 & + \int_0^a \frac{2\varepsilon_0(a-x)dx}{h_a + \frac{h_d}{\varepsilon_d} + \frac{\varepsilon_s+1}{\varepsilon_s}\pi(b-3a+x) - 2\frac{\varepsilon_d-1}{\varepsilon_d}(b-3a+x)\arcsin\frac{h_b}{b-3a+x}} + \\
 & + \frac{2\varepsilon_0\varepsilon_d\varepsilon_sh_b}{\pi(\varepsilon_d+\varepsilon_s)} \left\{ \left(1 + \frac{\varepsilon_d\varepsilon_s}{\pi(\varepsilon_d+\varepsilon_s)} \frac{\varepsilon_d h_a + h_d}{\varepsilon_d h_b} \right) \ln \left[1 + \frac{\varepsilon_d + \varepsilon_s}{\varepsilon_s} \frac{\pi h_b}{\varepsilon_d h_a + h_d} \right] - 1 \right\} .
 \end{aligned}$$

The two-dimensional finite element numerical models [10] correspond to those illustrated in fig. 2, where the vertical extension is $3(h_b+h_a+h_d)$ above the backplate for the computation of the hole capacitance per unit length and $3(b-3a)$ above the backplate for the computation of the marginal capacitance per unit length.

Null and unitary potentials were considered on the diaphragm and hollow backplate electrodes, respectively, and homogeneous Neumann conditions were considered on the remaining boundaries, and the capacitance was evaluated both in terms of electric charge and electric energy.

The two-dimensional models for the computation of the capacitance per unit length resulted in the three-dimensional numerical approximations of the elementary capacitances as

$$C_{HOLE}/C_{hole} = 0.9824 \quad , \quad C_{MARG}/C_{marg} = 0.9457 \quad , \quad C_{CORNER}/C_{corner} = 0.9244 \quad ,$$

in comparison with the corresponding analytically computed values.

CONCLUSIONS

The effective capacitance of an integrated capacitive microphone was computed by a mixed analytical and finite element numerical approach. The relative increase in the value of the effective capacitance resulted as the corresponding corrections

$$\frac{C_{\text{analytical}} - C_{\text{approx}}}{C_{\text{approx}}} \cong 12.1\% \quad , \quad \frac{C_{\text{numerical}} - C_{\text{approx}}}{C_{\text{approx}}} \cong 9.3\% \quad .$$

The computed values of the effective capacitance give improved data as compared to published results, [1], and the proposed methods can be successfully applied to other similar structures.

ACKNOWLEDGEMENTS

Thanks are due to the staff of the Numerical Methods Laboratory, and to colleagues in the Group of Theoretical Electrical Engineering of the Electrical Engineering Department, "Politehnica" University of Bucharest.

REFERENCES

1. M. Pedersen, W. Olthuis, P. Bergveld, *High Performance Condenser Microphone with Fully Integrated CMOS Amplifier and DC–DC Voltage Converter*, IEEE JMEMS, Vol 7, No. 4, December 1998, pp. 387–394.
2. J. Bergqvist, J. Gobet, *Capacitive Microphone with a Surface Micromachined Backplate Using Electroplating Technology*, IEEE JMEMS, Vol 3, No. 2, June 1994, pp. 69–75.
3. Q. Zou, Z. Li, L. Liu, *Design and Fabrication of Silicon Condenser Microphone Using Corrugated Diaphragm Technique*, IEEE JMEMS, Vol.5, No.3, September 1996, pp. 197–204.
4. George Cătălin Cazangiu, *Microfon capacitiv integrat*, Graduation thesis, Department of Electrical Engineering, Polytechnic University of Bucharest, 2004.
5. J. Van Bladel, *Electromagnetic Fields*, McGraw-Hill Book Company, New York, 1964.
6. H.A. Haus, J.R. Melcher, *Electromagnetic Fields and Energy*, Prentice Hall, Englewood Cliffs, J.J., 1989.
7. Anca Tomescu, F.M.G. Tomescu, R. Mărculescu, *Bazele electrotehnicii – Câmp electromagnetic*, MatrixRom, Bucharest, 2002.
8. Anca Tomescu, F.M.G. Tomescu, *Bazele electrotehnicii – Sisteme electromagnetice (Lecture Notes)*, Department of Electronics and Telecommunications, Polytechnic University of Bucharest, 1996.
9. M.L. Smoleanski, *Tabele de integrale nedefinite*, Editura Tehnică, Bucharest, 1972.
10. Anca Tomescu, I.B.L. Tomescu, F.M.G. Tomescu, *Modelarea numerică a câmpului electromagnetic*, MatrixRom, Bucharest, 2003.